Detector set up for the measurements of the neutron-induced fission cross section of ^{235}U relative to n-p scattering up to 150 MeV at CERN-n_TOF

E. Pirovano[1,*], *A.* Manna[2,3], *N.* Colonna[4], *P.* Console Camprini[2,5], *L.* Cosentino[6], *M.* Dietz[1], *Q.* Ducasse[1], *P.* Finocchiaro[6], *C.* Massimi[2,3], *A.* Mengoni[2,5], *R.* Nolte[1], *D.* Radeck[1], *L.* Tassan-Got[8,9,10], *N.* Terranova[7], *A.* Ventura[2], *O.* Aberle[8], *V.* Alcayne[11], *S.* Amaducci[6,12], *J.* Andrzejewski[13], *L.* Audouin[10], *V.* Babiano-Suarez[14], *M.* Bacak[8,15,16], *M.* Barbagallo[8,4], *S.* Bennett[17], *E.* Berthoumieux[16], *J.* Billowes[17], *D.* Bosnar[18], *A.* Brown[19], *M.* Busso[20,21], *M.* Caamaño[22], *L.* Caballero-Ontanaya[14], *F.* Calviño[23], *M.* Calviani[8], *D.* Cano-Ott[11], *A.* Casanovas[23], *F.* Cerutti[8], *E.* Chiaveri[8,17], *G.* Cortés[23], *M. A.* Cortés-Giraldo[24], *S.* Cristallo[20,25], *L. A.* Damone[4,26], *P. J.* Davies[17], *M.* Diakaki[9,8], *C.* Domingo-Pardo[14], *R.* Dressler[27], *E.* Dupont[16], *I.* Durán[22], *Z.* Eleme[28], *B.* Fernández-Domínguez[22], *A.* Ferrari[8], *K.* Göbel[29], *R.* Garg[30], *A.* Gawlik-Ramięga[13], *S.* Gilardoni[8], *I.* F. Gonçalves[31], *E.* González-Romero[11], *C.* Guerrero[24], *F.* Gunsing[16], *H.* Harada[32], *S.* Heinitz[27], *J.* Heyse[33], *D.* G. Jenkins[19], *A.* Junghans[34], *F.* Käppeler[†35], *Y.* Kadi[8], *A.* Kimura[32], *I.* Knapová[36], *M.* Kokkoris[9], *M.* Krtička[36], *D.* Kurtulgil[29], *I.* Ladarescu[14], *C.* Lederer-Woods[30], *H.* Leeb[15], *J.* Lerendegui-Marco[24], *S.* J. Lonsdale[30], *D.* Macina[8], *T.* Martínez[11], *A.* Masi[8], *P.* Mastinu[37], *M.* Mastromarco[8], *E. A.* Maugeri[27], *A.* Mazzone[4,38], *E.* Mendoza[11], *V.* Michalopoulou[9,8], *P. M.* Milazzo[39], *F.* Mingrone[8], *J.* Moreno-Soto[16], *A.* Musumarra[6,40], *A.* Negret[41], *F.* Ogállar[42], *A.* Oprea[41], *N.* Patronis[28], *A.* Pavlik[43], *J.* Perkowski[13], *L.* Piersanti[4,20,25], *C.* Petrone[41], *I.* Porras[42], *J.* Praena[42], *J. M.* Quesada[24], *D.* Ramos-Doval[10], *T.* Rauscher[44,45], *R.* Reifarth[29], *D.* Rochman[27], *C.* Rubbia[8], *M.* Sabaté-Gilarte[24,8], *A.* Saxena[46], *P.* Schillebeeckx[33], *D.* Schumann[27], *A.* Sekhar[17], *A. G.* Smith[17], *N. V.* Sosnin[17], *P.* Sprung[27], *A.* Stamatopoulos[9], *G.* Tagliente[4], *J. L.* Tain[14], *A.* Tarifeño-Saldivia[23], *Th.* Thomas[29], *P.* Torres-Sánchez[42], *A.* Tsinganis[8], *J.* Ulrich[27], *S.* Urlass[34,8], *S.* Valenta[36], *G.* Vannini[2,3], *V.* Variale[4], *P.* Vaz[31], *D.* Vescovi[20], *V.* Vlachoudis[8], *R.* Vlastou[9], *A.* Wallner[47], *P. J.* Woods[30], *T.* Wright[17], and *P.* Žugec[18]

[1]Physikalisch-Technische Bundesanstalt (PTB), Braunschweig, Germany
[2]Istituto Nazionale di Fisica Nucleare, Sezione di Bologna, Italy
[3]Dipartimento di Fisica e Astronomia, Università di Bologna, Italy
[4]Istituto Nazionale di Fisica Nucleare, Sezione di Bari, Italy
[5]Agenzia nazionale per le nuove tecnologie (ENEA), Bologna, Italy
[6]INFN Laboratori Nazionali del Sud, Catania, Italy
[7]Agenzia nazionale per le nuove tecnologie (ENEA), Frascati, Italy
[8]European Organization for Nuclear Research (CERN), Switzerland
[9]National Technical University of Athens, Greece
[10]Institut de Physique Nucléaire, CNRS-IN2P3, Univ. Paris-Sud, Université Paris-Saclay, F-91406 Orsay Cedex, France
[11]Centro de Investigaciones Energéticas Medioambientales y Tecnológicas (CIEMAT), Spain
[12]Dipartimento di Fisica e Astronomia, Università di Catania, Italy
[13]University of Lodz, Poland
[14]Instituto de Física Corpuscular, CSIC - Universidad de Valencia, Spain
[15]TU Wien, Atominstitut, Wien, Austria
[16]CEA Irfu, Université Paris-Saclay, F-91191 Gif-sur-Yvette, France
[17]University of Manchester, United Kingdom
[18]Department of Physics, Faculty of Science, University of Zagreb, Zagreb, Croatia
[19]University of York, United Kingdom
[20]Istituto Nazionale di Fisica Nucleare, Sezione di Perugia, Italy
[21]Dipartimento di Fisica e Geologia, Università di Perugia, Italy
[22]University of Santiago de Compostela, Spain
[23]Universitat Politècnica de Catalunya, Spain
[24]Universidad de Sevilla, Spain
[25]Istituto Nazionale di Astrofisica - Osservatorio Astronomico di Teramo, Italy
[26]Dipartimento Interateneo di Fisica, Università degli Studi di Bari, Italy
[27]Paul Scherrer Institut (PSI), Villigen, Switzerland
[28]University of Ioannina, Greece
[29]Goethe University Frankfurt, Germany
[30]School of Physics and Astronomy, University of Edinburgh, United Kingdom
[31]Instituto Superior Técnico, Lisbon, Portugal
[32]Japan Atomic Energy Agency (JAEA), Tokai-Mura, Japan
[33]European Commission, Joint Research Centre (JRC), Geel, Belgium

[34]Helmholtz-Zentrum Dresden-Rossendorf, Germany
[35]Karlsruhe Institute of Technology, Campus North, IKP, 76021 Karlsruhe, Germany
[36]Charles University, Prague, Czech Republic
[37]INFN Laboratori Nazionali di Legnaro, Italy
[38]Consiglio Nazionale delle Ricerche, Bari, Italy
[39]Istituto Nazionale di Fisica Nucleare, Sezione di Trieste, Italy
[40]Dipartimento di Fisica e Astronomia, Università di Catania, Italy
[41]Horia Hulubei National Institute of Physics and Nuclear Engineering, Romania
[42]University of Granada, Spain
[43]University of Vienna, Faculty of Physics, Vienna, Austria
[44]Department of Physics, University of Basel, Switzerland
[45]Centre for Astrophysics Research, University of Hertfordshire, United Kingdom
[46]Bhabha Atomic Research Centre (BARC), India
[47]Australian National University, Canberra, Australia

Abstract. A new measurement of the ^{235}U(n,f) fission cross section was carried out at n_TOF. The experiment covered the neutron energy range from 10 MeV up to 500 MeV, and it used the ^{1}H(n,n) cross section as normalization for the neutron fluence measurement. In this contribution, the measurements and the characterization of the detectors covering the incident energy range up to 150 MeV are discussed.

1 Introduction

The fission cross section of ^{235}U is a neutron cross section standard at the thermal neutron energy point (0.025 eV), and from 0.15 MeV to 200 MeV [1]. It is one of the few standards to extend to energies above 20 MeV, and it is therefore crucial for measurements of high-energy neutrons, with applications that range from the investigation of the biological effectiveness of high-energy neutrons, to the measurement of neutron cross-sections of relevance for advanced nuclear technologies such as accelerator-driven systems. Above 50 MeV, however, the cross-section evaluation recommended by the International Atomic Energy Agency (IAEA) is based on only two measurements, while above 200 MeV no experimental data are available. Hence, there is a clear and long-standing demand from the IAEA to improve this situation between 20 MeV and 1 GeV. In particular, there is a request [2] for new fission experiments to be performed relative to n-p elastic scattering, which is the primary reference for neutron cross-section measurements.

A new measurement of the ^{235}U(n,f) cross section relative to ^{1}H(n,n) was therefore carried out at n_TOF [3], the neutron time-of-flight facility of CERN, which is the only facility in Europe that can reach those energies. For the experimental setup, two lines of development were followed: one aimed at the improvement of the current standard evaluation [1], and the other at its extension above 200 MeV. In this contribution, the first approach will be presented, while the second is discussed in the paper by A. Manna *et al.* [4].

2 The experimental setup

The experimental set up was installed at the Experimental Area 1 (EAR1) of n_TOF, at a distance of about 183 m from the spallation target, where the neutron energy distribution extends from thermal energies up to 1 GeV. It consisted of ten ^{235}U samples mounted in two reaction chambers, and two polyethylene samples, which were all irradiated simultaneously by the neutron beam. This is schematically shown in figure 1.

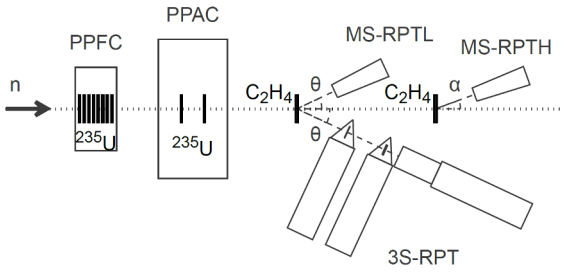

Figure 1. Representation of the experimental setup. Eight ^{235}U samples were installed in the PPFC, two were in the PPAC. One 3S-RPT and two MS-RPTs were used to identify protons emitted by two polyethylene samples at the laboratory angles $\theta = 25°$ (upstream sample) and $\alpha = 20°$ (downstream sample).

The fission fragments were detected using a Parallel-Plate Fission Chamber (PPFC) and a reaction chamber based on Parallel-Plate Avalanche Counters (PPAC). The recoil protons produced by neutrons scattering on the hydrogen nuclei in the polyethylene targets were identified using particle telescopes and the ΔE-E technique. Three Recoil Proton Telescopes (RPTs), of which two were Multiple-Stage telescopes (MS-RPTs) and one was a Triple-Stage telescope (3S-RPT), were placed outside the beam at the proton emission angles of 20 and 25 degrees.

The PPAC measurements covered the incident neutron energy range from the thermal point to 1 GeV, the MS-RPTs from 10 MeV up to 500 MeV. Their principle of operation and characterization is described in the contribution of A. Manna *et al.*. Here, the PPFC and the 3S-RPT are discussed. The neutron energy range of these two detectors was more limited: for the PPFC it went from the thermal point to 150 MeV, while for the 3S-RPT it started at about 30 MeV and ended at 150 MeV. However they offered other advantages; for example, the detection efficiency of the PPFC is close to unit and can be

*e-mail: elisa.pirovano@ptb.de

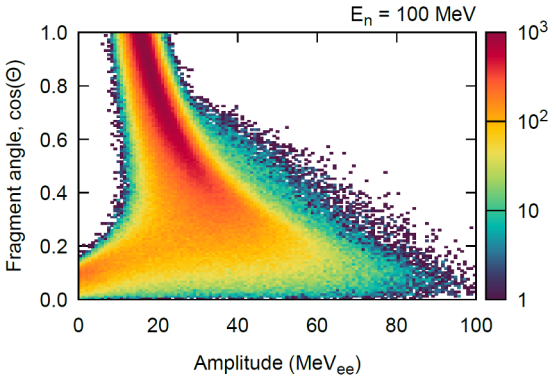

Figure 2. Results of the Monte Carlo model used to determine the efficiency of the PPFC. The figure shows the distribution of the fission fragments, the signal amplitude induced on the anode by the drifting electrons and their emission angle with respect to the incident neutron beam direction, obtained for an uranium sample with nominal mass of 295 μg/cm^2 and a neutron energy of 100 MeV.

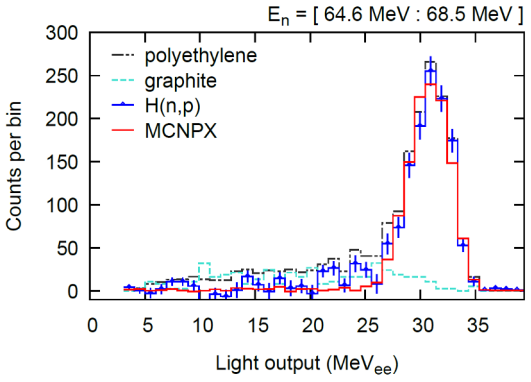

Figure 3. Light output distribution recorded by the stop detector of the 3S-RPT for incident neutrons with energy from 64.6 MeV to 68.5 MeV. The RPT telescope was composed by two transmission detectors of 1 mm thickness, and the stop detector was 5 cm long. The 'polyethylene' data were collected during a run with a polyethylene sample of 2 mm thickness, the 'graphite' data with a graphite sample of 1 mm thickness, and the 'H(n,p)' histogram is the results of the subtraction of the graphite events from the polyethylene events. The 'MCNPX' histogram shows the result of fitting the MCNPX simulation to the measurements.

calculated easily, and the 3S-RPT is characterized by excellent background suppression capabilities and provides a clear signature for recoil proton events. Moreover, having different detectors measuring the same quantities simultaneously allowed the early-on identification of systematic effects and it was critical for the assessment of the uncertainties.

3 Parallel-Plate Fission Chamber

The PPFC consisted of a stack of eight ^{235}U samples with a diameter of 42.00(3) mm, enriched with ^{235}U to the 99.9336(14) % in weight, and with mass per unit area ranging from 264 μg/cm^2 to 372 μg/cm^2. The chamber design aimed at reducing the amount of mass intercepting the neutron beam, to minimize the interaction with the gamma flash and avoid saturation effects caused by the high instantaneous neutron flux. The aluminum backings of the uranium targets were therefore only 30 μm thick, while for the entrance and exit windows, Kapton foils of 50 μm thickness were used. Despite the low total mass, the presence of aluminum is what determined the detection limit at a neutron energy of 150 MeV; above that energy events induced by reaction products from the aluminum backings started to interfere with fission events.

The fissile samples were manufactured at the EC Joint Research Centre in Geel (JRC-Geel) via molecular plating, where the uranium mass was measured by alpha counting and the isotopic composition by mass spectrometry. Detailed information on the chemical composition and the morphology of the layers are given in [5] for samples produced following the same method. The uniformity of the layers was determined at the Physikalisch-Technische Bundesanstalt (PTB) where autoradiographies of all samples were produced with phosphor imaging plates.

The efficiency of the PPFC was calculated using the information of the composition and morphology of the samples, and the experimental data on the angular distributions of the fission fragments measured for incident neutron energies from 20 MeV to 200 MeV [6–8]. Fission fragments traveling almost parallel to the fissile layers lose most of their kinetic energy before reaching the active volume of the detector, and do not produce a measurable signal. A dedicated Monte Carlo code was therefore developed to model the transport of the fission fragments inside the fissile layers, to determine how much energy is deposited in the layers and how much in the counting gas (see figure 2). This was used to calculate, as a function of the incident neutron energy, the amount of fission fragments stopped by the deposits, and the expected pulse-height distribution produced by the fragments reaching the counting gas. The energy-dependent pulse-height distributions were then fit to the experimental data to extrapolate the number of fission events below the threshold used to discriminate fission fragments from alpha particles.

4 The Triple-Stage Recoil Proton Telescope

The 3S-RPT was composed by two thin transmission detectors and a thick stop detector, all EJ-204 plastic scintillators. To identify particles emitted by the polyethylene samples, and to obtain a strong background suppression, only signals produced in triple coincidence were selected. To discriminate between protons and deuterons, the ΔE-E technique was used; while the separation of recoil protons from n-p scattering and protons from neutron reactions on carbon was achieved by subtracting the events measured during dedicated runs with graphite samples.

Several combinations of detectors and polyethylene samples of different thicknesses were used to extend the energy range of the detected recoil protons. Thin samples (down to 1 mm) and thin detectors (0.5 mm for the transmission detectors, 5 cm for the stop detector) were neces-

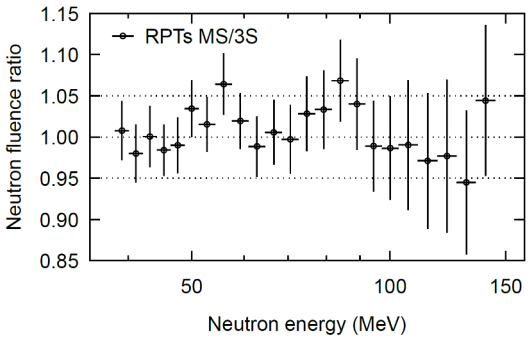

Figure 4. Ratio of the fluence reconstructed by the upstream MS-RPT to that of the 3S-RPT, preliminary results. The error bars represent the statistical uncertainty on the measurements of the single detectors.

sary to detect low-energy protons. To increase the counting statistics at higher energies, and for easier particle identification (larger energy deposition and light-output signals), thick samples (up to 5 mm) and thick detectors (up to 2 mm for the transmission detectors, 10 cm for the stop detector) were employed. In the granted beamtime, it was eventually possible to cover proton energies from 25 MeV to 120 MeV, which corresponded to incident neutron energies from 30 MeV to 150 MeV.

The polyethylene sample density was measured at PTB via hydrostatic weighing. Their lateral profile was also characterized at PTB, using two touch probes and a measuring stand to measure the samples from both sides simultaneously. The uncertainty on the areal density obtained from those measurements ranged from 0.2 % to 0.6 %, depending on the sample. The mass ratio of hydrogen and carbon in the samples was measured via combustion analysis by the ZEA-3 unit at the Forschungszentrum Jülich and the Institute for Inorganic and Analytical Chemistry at the Technische Universität Braunschweig. The ratio H:C was then found to be 1.98(3) and 2.00(3), i.e. compatible with the nominal value for polyethylene.

The proton detection efficiency of the 3S-RPT was calculated using MCNPX. The model included a detailed description of telescope geometry and of the sample composition. Nuclear data for neutron and proton-induced nuclear reactions were taken from the LA150 library [9] which extends up to 150 MeV and contains tabular data for all relevant materials, including the current standard evaluation for the ^{1}H(n,n)p cross section. The main drawback of MCNPX is that, to be consistent with the ENDF-6 format, it uses non-relativistic kinematics. For instance, the differential cross section n-p scattering was transformed from the center-of-mass system to the laboratory system using non relativistic equations. Above 20 MeV the effect on the expected counting rates is non negligible, and therefore it was corrected using analytical calculations based on kinematics.

Figure 3 shows the fit of the simulations to the experimental data for a given incident neutron energy bin. The histograms represent the light output distributions recorded by the stop detector during the runs with the polyethylene and graphite samples, and the result of the carbon subtraction. The corresponding MCNPX simulated distribution was fit to the experimental data to reconstruct the number of neutron incident on the polyethylene sample considering the exact geometry of the set up, the angular and the energy spread of the protons interacting with the material on the line of view.

5 Comparison of detectors and conclusions

The main strength of the experiment for the determination of the ^{235}U(n,f) cross section at high energies was the presence of detectors based on different concepts measuring the same quantities simultaneously.

For example, figure 4 shows the ratio of the incident neutron fluence reconstructed by the upstream MS-RPT to that of the 3S-RPT. A similar comparison is also currently ongoing for the second MS-RPT, the PPAC and the PPFC. The error bars were calculated from the statistical uncertainties, which ranged from 5 % to 10 %, depending on the detector and the energy range. The uncertainties on the combined results should be substantially reduced. The good compatibility between measurements is the result of the detailed study of the detection efficiency. Eventual residual discrepancies would nevertheless provide valuable information, as they could be used to determine, in a quantitative way, potentially unknown systematic uncertainties.

The cross-checks between different systems allowed to build confidence on the results below and above 200 MeV, which will presumably have a positive impact both on the existing standard evaluation and to its extension to higher energies.

Acknowledgements

In line with the principles that apply to scientific publishing and the CERN policy in matters of scientific publications, the n_TOF Collaboration recognises the work of V. Furman and Y. Kopatch (JINR, Russia), who have contributed to the experiment used to obtain the results described in this paper.

References

[1] A. D. Carlson *et al.*, Nucl. Data Sheets **148**, 143-188 (2018)
[2] B. Marcinkevicius *et al.*, INDC(NDS)-0681 (2015)
[3] C. Borcea *et al.*, Nucl. Instrum. and Methods in Phys. Res. A **513**, 524-537 (2003)
[4] A. Manna et. *et al.*, To be published in EPJ Web of Conferences ND2022 proceedings, 2023
[5] G. Sibbens *et al.*, AIP Conference Proceedings **1962**, 030007 (2018)
[6] A. S. Vorobeyev *et al.*, Eur. Phys. J. Web of Conf. **146**, 04011 (2017)
[7] V. Geppert-Kleinrath *et al.*, Phys. Rev. C **99**, 064619 (2019)

[8] E. Leal-Cidoncha *et al.*, Eur. Phys. J. Web of Conf. **111**, 10002 (2016)

[9] M. B. Chadwick *et al.*, Nucl. Sci. Eng. **131**, 293-329 (1999)